Infrared-active phonons of $LaMnO_3$ and $CaMnO_3$

I. Fedorov, J. Lorenzana,* P. Dore, G. De Marzi, P. Maselli, and P. Calvani
Istituto Nazionale di Fisica della Materia–Dipartimento di Fisica, Università di Roma ''La Sapienza,'' Piazzale Aldo Moro 2, I-00185 Roma, Italy

S.-W. Cheong
Bell Laboratories, Lucent Technologies, Murray Hill, New Jersey 07974 and Department of Physics, Rutgers University, Piscataway, New Jersey 08855

S. Koval and R. Migoni
Instituto de Fisica Rosario, Universidad Nacional de Rosario, 2000 Rosario, Argentina
(Received 6 November 1998; revised manuscript received 7 May 1999)

The infrared absorption spectra of polycrystalline $LaMnO_3$ and $CaMnO_3$ measured in the frequency range of the transverse optical phonons are reported, discussed, and compared with calculations of the lattice dynamics. For $LaMnO_3$ the measured spectrum is consistent with the expected orthorhombic structure. For $CaMnO_3$ the spectrum reflects a symmetry lower than that of a cubic perovskite. We find a close correspondence between the spectra of the two materials which suggests a similarity in their structures. [S0163-1829(99)09441-2]

Recently, the $La_{1-x}Ca_xMnO_3$ system has stimulated considerable interest because of its colossal magnetoresistance.[1,2] The phase diagram of $La_{1-x}Ca_xMnO_3$ reveals a variety of ground states, depending on the carrier concentration x.[3] For $0.2 \leqslant x \leqslant 0.48$, the system undergoes coincident metal-insulator and ferromagnetic-paramagnetic transitions at $T \lesssim 250$ K. Out of this range of x, insulating ground states with different types of magnetic ordering take place.[3] The coexistence of ferromagnetic ordering and metallic transport was successfully explained several decades ago by the double exchange model.[4] A more recent theory that accounts quantitatively for the colossal magnetoresistance phenomenon[5] implies a strong electron-phonon coupling. While the spectrum of electronic excitations has been thoroughly studied,[6,7] little is known about the phonons of $La_{1-x}Ca_xMnO_3$. Obtaining information about the optical phonons of the end-member compounds $LaMnO_3$ and $CaMnO_3$ may greatly help in further studies of the doping and temperature dependence of the phonon modes in $La_{1-x}Ca_xMnO_3$ and of their interplay with the magnetoresistance effects.

The structure of $LaMnO_3$ was determined using neutron[8] and x-ray[9] diffraction. Below ~ 800 K, $LaMnO_3$ was found to have an orthorhombic structure ($Pnma$ space group).[8] The deviation of the structure from cubic is usually attributed to the Jahn-Teller instability of the Mn^{3+} ion.[3] The Raman-active phonons in $LaMnO_3$ were studied at room temperature by Iliev *et al.*[10] The assignment of the observed Raman peaks was done by comparison of the experimental data with the results of lattice dynamical calculations (LDC). Consistent results were obtained by Granado *et al.*,[11] who recently reported the temperature dependence of the $LaMnO_3$ Raman spectrum between 300 and 10 K. Up to now, there has not been any systematic study of the infrared-active phonons in $LaMnO_3$, at least to our knowledge. The infrared absorption spectra of polycrystalline $LaMnO_3$ reported in an earlier work[12] do not allow to determine most phonon frequencies. Recently, Jung *et al.*[7] have presented reflectivity spectra of polycrystalline $La_{1-x}Ca_xMnO_3$ measured from 5 meV up to 30 eV for different values of x (including $x=0$ and $x=1$), but the authors do not analyze the phonon part of the spectra. Concerning $CaMnO_3$, we are not aware of any neutron-diffraction study of the structure of this material. Available x-ray-diffraction data point towards an orthorhombic structure.[13] This compound is thought to have a structure much closer to cubic than $LaMnO_3$ as the Mn^{4+} ion does not produce any Jahn-Teller distortion.[3] The Raman-active phonons of $CaMnO_3$ have never been reported in the literature, whereas the published infrared data [7,13] have not been discussed.

In this paper we report measurements of the infrared-active phonons in polycrystalline $LaMnO_3$ and $CaMnO_3$. We present a comparative analysis of the infrared spectra of these compounds and we propose an assignment for the observed phonon modes based on calculations of the lattice dynamics.

Polycrystalline powders of $LaMnO_3$ and $CaMnO_3$ were synthesized by a standard solid-state reaction method as described in Ref. 2. Powder x-ray-diffraction analysis showed that the samples had single-phase orthorhombic structures. The oxygen stoichiometry has been accurately controlled within 0.5%. The powders were finely milled, mixed with CsI (in the ratio 1:100 in weight), and pressed into pellets under vacuum. The infrared optical density $O_d(\omega)$ for both compounds was obtained in the 150–650-cm^{-1} frequency range at 300, 200, 100, and 20 K using a Fourier spectrometer. At each temperature we measured the ratio $I(\omega)/I_0(\omega)$ of the infrared signal transmitted by the CsI pellets containing the samples and that transmitted by a pure CsI pellet. $O_d(\omega)$ was then obtained as $-\ln(I(\omega)/I_0(\omega))$. The experimental resolution was 5 cm^{-1}. It should be noted that we were not able to extend our measurements below 150 cm^{-1} because CsI is opaque at low frequencies.[14] The infrared optical densities of polycrystalline $LaMnO_3$ and $CaMnO_3$ at

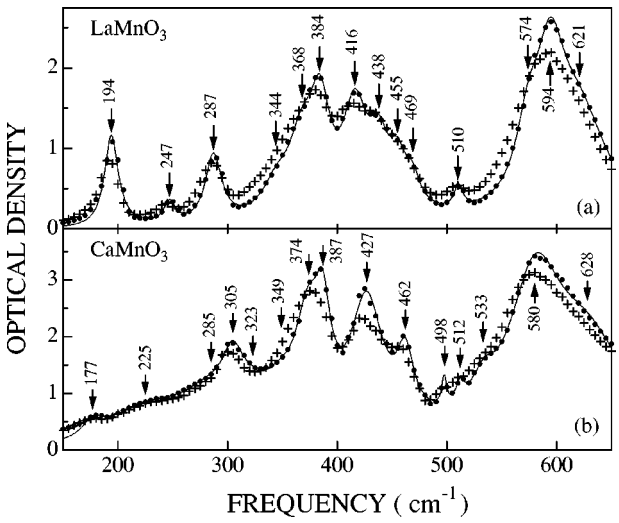

FIG. 1. Optical density of polycrystalline $LaMnO_3$ (a) and $CaMnO_3$ (b) measured at 20 K (dots) and 300 K (+). The solid curves represent the best fit of the 20 K data according to Eq. (1). The phonon frequencies thus obtained are also reported.

300 and 20 K are shown in Figs. 1(a) and 1(b), respectively. It is evident that the spectra do not show significant temperature dependence.[15] In particular we did not observe significant shifts in the phonon peak positions within our resolution. Small shifts were found for some Raman-active phonons in the mentioned measurements by Granado *et al.*[11] that were performed with a resolution better than that in our experiments. In the following, we shall focus on the 20 K spectra as the phonon peaks are better resolved at low temperatures.

The spectra exhibit numerous peaks associated with the infrared active transverse-optical (TO) modes. The large number of modes indicates strong deviations from a cubic symmetry in both compounds. Above ~ 270 cm^{-1}, the spectra of Figs. 1(a) and 1(b) appear to be very similar. As it is discussed below, this can be explained by the fact that the high-frequency phonons involve mostly motions of the oxygen octahedra. To extract information about phonons we fitted the spectra of Fig. 1 using a sum of noninteracting harmonic oscillators (Lorentz model). It was shown earlier[14] that in the first approximation $O_d(\omega) \propto \sigma_1(\omega)$, where $\sigma_1(\omega)$ is the optical conductivity. Taking this into account, we can write[16]

$$O_d(\omega) = \sum_j \frac{S_j \omega^2 \gamma_j}{(\omega_j^2 - \omega^2)^2 + \gamma_j^2 \omega^2}, \tag{1}$$

where ω_j, γ_j, and S_j are the frequency, width and amplitude of the TO jth oscillator, respectively. The minimum number of oscillators that allow us to obtain a reliable fit is 14 for $LaMnO_3$ and 15 for $CaMnO_3$. In Fig. 1, the solid lines illustrate the accuracy of the fit and the resulting phonon frequencies ω_j are shown. For $LaMnO_3$, we report in Table I the values of ω_j and γ_j for each peak. We also give the relative weights A_j obtained through

$$A_j = \frac{100 S_j}{\sum S_i}. \tag{2}$$

TABLE I. Phonon assignment for $LaMnO_3$. In the first three columns the best-fit values of the frequencies (ω_j), dampings (γ_j), and amplitudes (A_j) of the measured phonon peaks are given. The last three columns represent the results of LDC for $LaMnO_3$. ω_j and γ_j are in cm^{-1}, the A_j are dimensionless [see Eq. (2)].

Best fit			LDC		
ω_j	γ_j	A_j	ω_j	A_j	Symmetry
			76	1.1	B_{1u}
			117	$\sim 10^{-4}$	B_{3u}
			191	$\sim 10^{-3}$	B_{2u}
194	15	5.4	194	2.5	B_{1u}
247	13	1.0	233	0.2	B_{2u}
			233	0.1	B_{3u}
			273	7.1	B_{1u}
			276	3.3	B_{3u}
			283	$\sim 10^{-3}$	B_{2u}
287	18	4.8	294	13.4	B_{3u}
			318	0.8	B_{1u}
344	32	3.6	332	7.8	B_{3u}
			334	3.1	B_{1u}
368	32	9.1	388	6.0	B_{2u}
384	22	7.2	401	13.2	B_{3u}
416	28	11.1	412	9.7	B_{2u}
			419	7.2	B_{1u}
438	22	5.0	431	12.1	B_{1u}
455	19	3.0	443	5.7	B_{3u}
469	17	1.8	495	1.0	B_{1u}
510	10	0.8	521	0.4	B_{3u}
574	28	6.9	577	3.4	B_{1u}
			580	0.1	B_{2u}
594	33	15.9	580	0.8	B_{3u}
621	64	24.4	625	1.0	B_{2u}

In order to assign the observed phonon peaks we performed calculations of the lattice dynamics following the procedure described in Refs. 17 and 18. This approach is based on the use of a shell model and provides information about the phonon frequencies and the corresponding atomic displacements. We restricted our calculations to the Γ point of the Brillouin zone ($k \approx 0$). For $LaMnO_3$, both the lattice constants and the atomic positions were taken from neutron-diffraction data,[8] and the shell-model parameters from Ref. 17. In agreement with the group theory analysis performed in Ref. 10, we obtained 60 phonon modes, of which 24 are Raman active ($7A_g + 5B_{1g} + 7B_{2g} + 5B_{3g}$), 25 are infrared-active ($9B_{1u} + 7B_{2u} + 9B_{3u}$), 8 are silent ($8A_u$), and 3 are acoustic ($B_{1u} + B_{2u} + B_{3u}$). The infrared-active (TO) phonons of B_{1u}, B_{2u}, and B_{3u} symmetry correspond to oscillations of the dipole moment along the z, y, and x direction, respectively (x,y,z are defined as in Ref. 10). To check the validity of our results we compared the calculated frequencies and symmetries of the Raman-active phonons with those presented in Ref. 10 and we found good agreement between two sets of data. For each mode we also calculated the oscillator strength S_j using the formalism of Ref. 18. To allow a direct comparison with the experimental results, the relative weight A_j of each TO mode was estimated according to Eq. (2). In Fig. 2 we show some selected TO phonon modes.

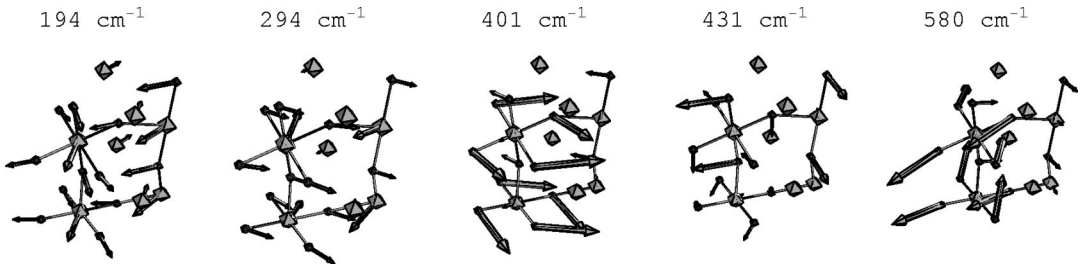

FIG. 2. Selected phonon modes labeled by the theoretical frequency. Isolated polyhedra represent the La atoms. Joined polyhedra represent the Mn (big) and O (small) atoms. The arrows represent the atomic displacements.

As our measurements were performed on polycrystalline samples, we cannot distinguish the contributions from different crystal axes. For this reason, no information about the symmetries of the phonon peaks can be extracted from the experimental data, and we made the assignment by comparing the phonon frequencies obtained from the fit with those found in LDC. The results of this comparison are summarized in Table I. Inspection of Table I shows that some of the experimentally observed peaks cannot be assigned unambiguously. For example, the peak at 416 cm^{-1} could be associated either with the B_{2u}-symmetry phonon mode expected at 412 cm^{-1} or with the B_{1u}-symmetry mode at 419 cm^{-1}. In all cases when such an ambiguity appeared, we assigned the measured peak in optical density to the calculated phonon mode with the largest amplitude. It should be noted that the experimental values of A_j are in fair agreement with the results of LDC, except for the modes at 594 and 621 cm^{-1}, whose calculated amplitudes appear to be about one order of magnitude lower than the experimental ones. The results of Ref. 7 are in qualitative agreement with our data, suggesting that LDC does not account properly for the amplitude of the high-frequency modes. However, taking into account the complexity of this class of materials and the fact that we have not done any optimization of the shell model parameters, we believe that the overall agreement between theory and experiment should be considered as reasonable.

An attempt to perform calculations of the lattice dynamics of $CaMnO_3$ was frustrated by the exceedingly high number of unknown parameters. The lattice constants can be taken from x-ray-diffraction data,[13] but due to the lack of neutron data the exact atomic positions are not known. Moreover, the results of LDC are very sensitive to the manganese shell model parameters. In the $LaMnO_3$ case the Mn^{+3} shell model parameters are known,[17] while for $CaMnO_3$ the Mn^{+4} shell model parameters have not been reported in the literature. As it was mentioned above, there are evident similarities in both the positions and the shapes of the infrared phonon peaks of $CaMnO_3$ and $LaMnO_3$. Taking this into account, we made our (tentative) phonon assignment for $CaMnO_3$ using a simple correlation procedure. For each absorption peak in the infrared spectrum of $CaMnO_3$ we looked for a counterpart in the spectrum of $LaMnO_3$. The results of this procedure are reported in Table II. We did not assign the $CaMnO_3$ weak modes at 285 and 323 cm^{-1} as they do not appear in the spectrum of $LaMnO_3$ (they probably contribute to the broadening of the strong absorption peak at 287 cm^{-1}). On the other hand, the $LaMnO_3$ mode at 438 cm^{-1} does not have a counterpart in the $CaMnO_3$ spectrum where it is probably hidden by the intense peak at 427 cm^{-1}.

Let us now discuss within the present assignment the microscopic motions related to the observed phonon peaks in the infrared spectrum of $LaMnO_3$. In the following discussion we quote in brackets the theoretical frequencies of the modes displayed in Fig. 2. As shown in the figure the phonon mode at 194 (194) involve mixed vibrations of the La atoms and the MnO_6 octahedra. The same occurs for the mode at 247 cm^{-1}. These modes can be understood as the result of splitting of the lowest-frequency phonon of the ideal perovskite structure (external mode). It can be seen from Fig. 1 that substitution of the La atoms with Ca ones strongly affects both the modes which appear in the $CaMnO_3$ spectrum as broad and weak peaks. The higher frequency modes do not involve motions of La atoms. This fact explains the mentioned similarity between the infrared spectra of $LaMnO_3$ and $CaMnO_3$ above $\sim$270 cm^{-1}. As shown in Fig. 2 the mode at 287 (294), as well as the one at 344 cm^{-1}, correspond to complex motions, where the amplitudes of the displacements of the Mn atoms are comparable with those of the O atoms. On the other hand, in the mode at 368 cm^{-1} and in those at higher frequencies the oxygen motions dominate, so that for these modes the La and Mn atoms should be assumed to be at rest. For the modes at 368, 384 (401), 416, 510, 574, and 594 (580) cm^{-1} the in-plane oxygen vibrations dominate. For those at 438 (431), 455, and 621 cm^{-1} the motions of the apical oxygen atoms play the main role. Only for the mode at 469 cm^{-1} the amplitudes of the displacements of the in-plane O atoms are comparable with those of the apical O atoms. The group of phonons with frequencies lying between $\sim$270 and $\sim$550 cm^{-1} is expected to originate from splitting of the bending mode of the ideal perovskite structure. Similarly, the stretching mode of

TABLE II. Correspondence between the best fit phonon frequencies (in cm^{-1}) of $LaMnO_3$ and those of $CaMnO_3$.

$LaMnO_3$	194	247		287		344	368	384	416	438	455	469	510	574	594	621
$CaMnO_3$	177	225	285	305	323	349	374	387	427		462	498	512	533	580	628

the cubic crystal is assumed to give rise to the group of modes of orthorhombic symmetry whose frequencies exceed $\sim 550\ \mathrm{cm}^{-1}$. However, due to the strong orthorhombic lattice distortions, none of the modes observed above $\sim 270\ \mathrm{cm}^{-1}$ can be classified as purely bending or as purely stretching as these modes imply considerable changes of both the Mn–O–Mn bond angles and the Mn–O bond lengths.

In conclusion, we have reported the infrared absorption spectra of polycrystalline $LaMnO_3$ and $CaMnO_3$. Using calculations of the lattice dynamics and comparative analysis of the measured spectra we were able to propose a reasonable assignment for the phonon modes observed in $LaMnO_3$. The agreement found between theory and experiment allows us to confirm the orthorombic structural model of Ref. 8. For $CaMnO_3$ the high number of observed phonon modes rules out a simple cubic perovskite structure. The close similarity found between the spectra of the two materials suggest that their structures are similar. If this result is confirmed through specific structural analysis, it would imply that the Jahn-Teller effect is not the driving force of the orthorombic distortion, as it is absent in $CaMnO_3$.

It should be pointed out that further studies with polarized radiation on single-crystalline $LaMnO_3$ and $CaMnO_3$ (provided that single crystals suitable for far-infrared measurements become available) are highly desirable in order to remove the present ambiguities in the phonon assignment.

*Permanent address: Centro Atómico Bariloche (CONICET) and Instituto Balseiro, 8400 S. C. de Bariloche, Argentina.

[1] S. Jin, T. H. Tiefel, M. McCormack, R. A. Fastnacht, R. Ramesh, and L. H. Chen, Science **264**, 413 (1994).
[2] P. Schiffer, A. P. Ramirez, W. Bao, and S.-W. Cheong, Phys. Rev. Lett. **75**, 3336 (1995).
[3] A. J. Millis, Nature (London) **392**, 147 (1998).
[4] C. Zener, Phys. Rev. **82**, 403 (1951).
[5] A. J. Millis, P. B. Littlewood, and B. I. Shraiman, Phys. Rev. Lett. **74**, 5144 (1995).
[6] J. H. Jung, K. H. Kim, D. J. Eom, T. W. Noh, E. J. Choi, J. Yu, Y. S. Kwon, and Y. Chung, Phys. Rev. B **55**, 15 489 (1997).
[7] J. H. Jung, K. H. Kim, T. W. Noh, E. J. Choi, and J. Yu, Phys. Rev. B **57**, R11 043 (1998).
[8] J. Rodriguez-Carvajal, M. Hennion, F. Moussa, A. H. Moudden, L. Pinsard, and A. Revcolevschi, Phys. Rev. B **57**, R3189 (1998).
[9] J. A. M. van Roosmalen, P. van Vlaanderen, E. H. P. Cordfunke, W. L. Ijdo, and D. J. W. Ijdo, J. Solid State Chem. **114**, 516 (1995).
[10] M. N. Iliev, M. V. Abrashev, H.-G. Lee, V. N. Popov, Y. Y. Sun, C. Thomsen, R. L. Meng, and C. W. Chu, Phys. Rev. B **57**, 2872 (1998).
[11] E. Granado, N. O. Moreno, A. Garcia, J. A. Sanjurjo, C. Rettori, I. Torriani, S. B. Oseroff, J. J. Neumeier, K. J. McClellan, S.-W. Cheong, and Y. Tokura, Phys. Rev. B **58**, 11 435 (1998).
[12] G. V. Subba Rao, C. N. R. Rao, and J. R. Ferraro, Appl. Spectrosc. **24**, 436 (1970).
[13] K. R. Poeppelmeier, M. E. Leonowicz, and J. M. Longo, J. Solid State Chem. **44**, 89 (1982).
[14] A. Paolone, P. Giura, P. Calvani, P. Dore, S. Lupi, and P. Maselli, Physica B **244**, 33 (1998).
[15] P. Calvani, G. De Marzi, P. Dore, S. Lupi, P. Maselli, F. D'Amore, S. Gagliardi, and S.-W. Cheong, Phys. Rev. Lett. **81**, 4504 (1998).
[16] G. Burns, *Solid State Physics* (Academic Press, New York, 1985).
[17] V. N. Popov, J. Phys.: Condens. Matter **7**, 1625 (1995).
[18] S. Koval and R. Migoni, Phys. Rev. B **51**, 6634 (1995).